



Computer model of an aberrant right subclavian artery (arteria subclavia dextra lusoria)

Published online February 14th, 2017 © <http://www.ijav.org>Ali Cem KUCUKDAGLI^{[1]†}Kaori TAMURA^[2]Cris STICKLEY^[2]Trudy HONG^[3]Beth K. LOZANOFF^[3]Steven LABRASH^[3]Scott LOZANOFF^[3]

Class of 2015, Hacettepe University Faculty of Medicine, Ankara, TURKEY
 [1]: Department of Kinesiology and Rehabilitation Science [2], Department
 of Anatomy, Biochemistry & Physiology, John Burns School of Medicine [3],
 University of Hawaii at Manoa, Honolulu, HI, USA.



† Ali Cem Kucukdagli, MD

Dept. of Pediatrics
 Hacettepe University
 Faculty of Medicine
 Ankara, TURKEY.

☎ +90 (312) 305 11 95

✉ ceeems@hotmail.com

Received February 16th, 2015; accepted January 7th, 2017

Abstract

The aorta serves as the systemic outflow tract from the heart and it is subject to anatomical variation in the adult, in part, to a complicated set of temporospatial and morphogenetic interactions. The occurrence of an aberrant right subclavian artery (arteria subclavia dextra lusoria, ARSA) is reported to occur with a frequency of approximately 0.1-25.0%. We report the occurrence of ARSA in a cadaver from a 91-year-old male during a routine dissection of the thorax. Features included a bicarotid trunk, normal left subclavian, but a right subclavian that branched from the terminal portion of the descending aorta. The ARSA was positioned in a retroesophageal and retrotracheal location. However, the person was asymptomatic with respect to the ARSA during his life according to medical records. Animations were generated to demonstrate the spatial relationships of the ARSA in this individual. Additional animations were generated to depict embryological relationships that were likely associated with the formation of ARSA in this cadaver. To our knowledge, this is the first time an animation of ARSA has been presented.

© *Int J Anat Var (IJAV)*. 2016; 9: 95–99.**Key words** [aberrant right subclavian artery] [ARSA] [bicarotid trunk] [computer model] [computer animation of ARSA]

Introduction

The aorta serves as a primary outflow pathway for the heart and typically comprises ascending and descending components. At its origin, the aorta travels anterior to the trachea and esophagus, but arches and then descends to the left of these two structures. Primary branches include, progressing from right to left, the brachiocephalic trunk with common carotid and subclavian branches, left common carotid and left subclavian artery. This branching pattern is subject to anatomical variation, in part, due to complex developmental mechanisms that convert six bilateral embryological vessels to a reduced number of side-specific derivatives (Moes and Freedom, 1993). The right subclavian is particularly vulnerable to anatomical variation since it is derived as a composite structure including the aortic sac and fourth branchial arch artery as well as its eventual connection with third branchial arch artery and dorsal aorta (Knight and Edwards, 1974; Fazan et al., 2003; Davies and Guest, 2003; Tubbs et al., 2004; Saito et al., 2005; Chaoui et al., 2008). In a comprehensive survey, Natsis et al. (2009) provided a categorization of aortic arch variants. Type V was defined as an aberrant right subclavian artery (ARSA), or arteria subclavia dextra lusoria, that arises as the last branch

of the aorta with an incidence of 0.16% based on a sample from 633 angiographies. However, incidence can vary widely with values reported between 0.13% and 25% (Bergman et al., 1988). This variant is typically asymptomatic, but it is reported that approximately 10% of afflicted patients display dysphagia lusoria particularly when the ARSA runs posterior to the esophagus (Brown et al., 1993). These patients may also present with features consistent with tracheal compression including stridor, cyanosis and hoarseness (Donnelly et al., 2002; Chadha and Chtit-Batelli, 2004). Patients might be afflicted with a Kommerell's diverticulum (Nakatani et al., 1996; Yang et al., 2012) increasing the risk of complications consistent with aneurysms (Austin and Wolfe, 1985; Ilijevski et al., 2011) as well as the possibility of an ARSA-esophageal fistula (Miller et al., 1996) associated with ischemia and thrombosis (Boas et al., 2002).

ARSA has long been known and may have been first reported by Hanuld in 1735 as cited by Bergman et al. (1988). However, its occurrence with a bicarotid trunk is very uncommon (Rogers et al., 2011). An understanding of the morphology and spatial relationships of surrounding structures related to ARSA is important for the accurate assessment of related symptoms and clinical diagnosis of associated complications

(Epstein and DeBord, 2002). Advanced imaging methods within a clinical context have facilitated three-dimensional visualizations of cardiovascular components associated with ARSA (Turkenburg et al., 1994; Meier et al., 1993; Lee et al., 2004; Rogers et al., 2011). However, a rendering of ARSA within the context of contiguous anatomical structures for instructional purposes has not been provided. The purpose of this report is to describe the occurrence of ARSA with a bicarotid trunk as well as to present a QuickTime video for the appreciation of three-dimensional spatial relationships of ARSA for instructional applications.

Case Report

The ARSA was incidentally identified during routine anatomy dissection in the medical student instructional laboratory. The cadaver was that of a 91-year-old male. The ARSA and associated symptoms were not reported in the medical record suggesting the individual was asymptomatic. The typical features of the aortic cardiac outflow include the right innominate trunk with right subclavian and common carotid arterial branches followed by the left common carotid and left subclavian branches in sequence (Figure 1A). The atypical case shows a bicarotid trunk as the first branch followed by left and right subclavian arteries in sequence (Figure 1B). The overall cardiac morphology and spatial relationships were largely normal with heart positioned normally within the thorax and the ascending aorta arching posterosuperiorly curving to the left (Figure 2). Closer inspection revealed that the first branch was a bicarotid trunk (20 mm diameter) from which left and right common carotid arteries arose, each with initial diameters of 8 mm (Figures 2, 3). The second branch of the aorta was the left subclavian artery (10 mm in diameter) that continued superiorly into the left upper extremity. The third branch was the right subclavian that was positioned posterior to the trachea and esophagus and followed a retroesophageal (Figure 4) and retrotracheal (Figure 6) course. Following removal of the trachea and esophagus, the ARSA could be seen arising from the aorta at a right angle running horizontally (28 mm) and then turning sharply superior (Figure 6). This branch (69 mm) continued superiorly passing inferior to the clavicle and entering the upper extremity (Figure 6).

Animations were developed to facilitate understanding of the embryological basis of the case as well as the specific three-dimensional spatial relationships of thoracic viscera (Animations 1-4). The animations of the adult structures were based on the dissection, linear measurements and photographs. Wire mesh simulations were lofted using Maya (www.autodesk.com) and animated within the program to depict rotations around the Y-axis. The animation was rendered as a series of JPEG image files. The image sequence was opened in QuickTime Pro and then exported as a QuickTime movie. Subsequently, the model was loaded into Z-space (www.zspace.com) for 3D observation.

Embryologically, aortic arches 3, 4 and 5 as well as the right 7th intersegmental artery are primary components of ARSA

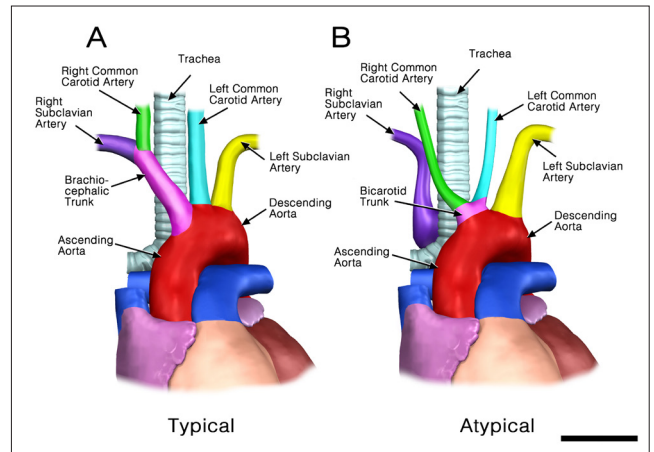


Figure 1. Computer model of (A) typical and (B) atypical ARSA outflow patterns of the heart and great vessels (A) and corresponding computer model (B) of viewed from the anterior perspective. Typically, the innominate artery with right common carotid and right subclavian branches occurs as the first tributary of the ascending aorta followed by the left common carotid and left subclavian branches in sequence. The atypical ARSA pattern displays a bicarotid trunk as the first component arising from the ascending aorta followed by a left subclavian artery and subsequently the ARSA following a route posterior to the trachea.

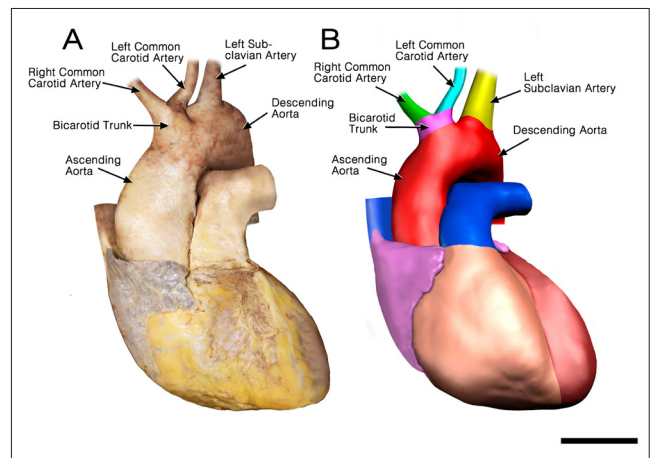


Figure 2. Photograph (A) computer model (B) demonstrating bicarotid trunk as the first branch and left subclavian artery as the second branch of the aortic arch viewed from the anterior perspective. Bar = 40 mm.

development (Animation 1). In ARSA, the proximal portion of the right dorsal aorta is lost while the dorsal portion, that typically obliterates, is retained (Animation 2). Similarly the right fourth aortic arch obliterates (Animation 2). As a result, the right intersegmental, that eventually gives rise to the subclavian artery, becomes absorbed into the dorsal aorta with its origin occurring distal to the left subclavian derived from the left 7th intersegmental artery (Animation 2). The right subclavian, in the case described her, looped posterior

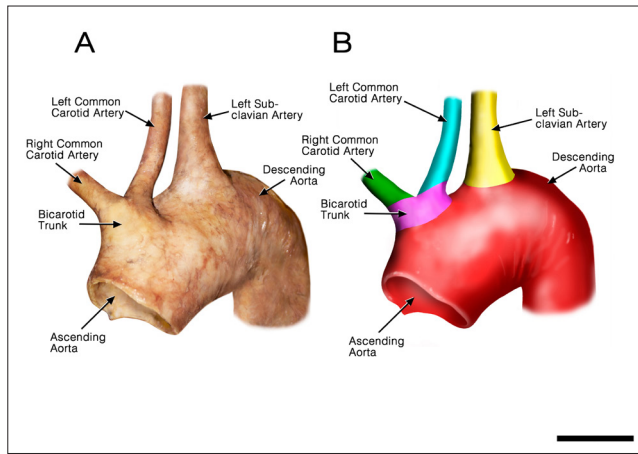


Figure 3. Photograph (A) computer model (B) demonstrating bicarotid trunk with left and right common carotid branches as the first tributary arising from the ascending aorta. Viewed from the anterior perspective and a higher magnification compared with Figure 2. Bar = 20 mm.

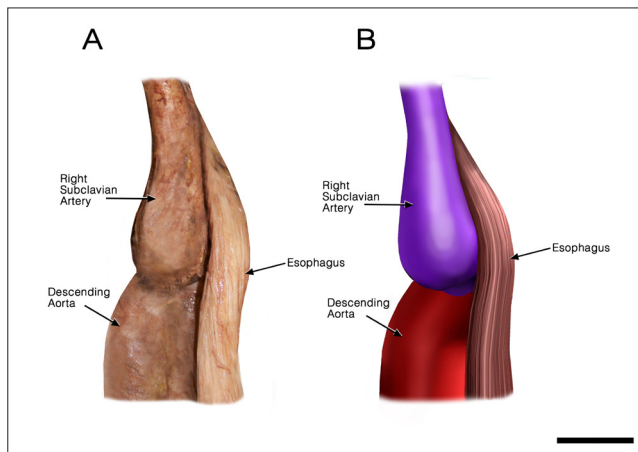


Figure 4. Photograph (A) and computer model (B) showing the right subclavian artery in a retroesophageal position and viewed from the right lateral perspective. The trachea is pulled forward and not included in this figure. Bar = 20 mm.

to the esophagus and trachea and the innominate artery does not form (Animations 3,4). Aortic arch 3 becomes absorbed into the dorsal aorta and the typical spatial arrangement of the common carotid arteries is lacking and a common bicarotid trunk results (Animations 2,3,4). The entire developmental process leading to an ARSA, thus, is driven primarily by an alteration of dorsal aortae obliteration (Animation 2,3,4).

Discussion

The development of the aortic arches occurs between approximately embryonic days 22-49 (Carnegie stages 11-20), as the dorsal aorta forms and subsequently, cardiac outflow transforms into the ascending aorta and its cardinal branches

(Congdon, 1922; O’Rahilly, 1971). The derivation of adult structures from aortic arch components is well known (Sadler, 2012). The brachiocephalic trunk arises from the aortic sac while the common carotids arise from the third arch and the right subclavian is derived, in part, from the right fourth aortic arch (Sadler 2012:185-191). It is believed that an ARSA arises as the last branch of the aorta when the distal portion of the fourth arch fails to involute and is retained (Davies and Guest, 2003). As a result, the right subclavian artery courses posterior to the trachea and esophagus. Simultaneously,

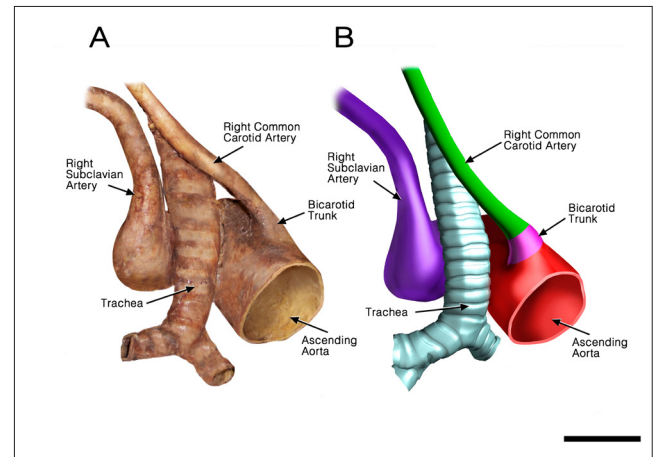


Figure 5. Photograph (A) and computer model (B) showing that the right common carotid artery arises separately from the aorta via a bicarotid trunk. The aberrant right subclavian artery demonstrates two right angle transitions, first from the aorta, and coursing posterior to the trachea and then ascending into the right upper extremity as viewed from the anterior perspective with the transected aorta reflected laterally. Bar = 20 mm.

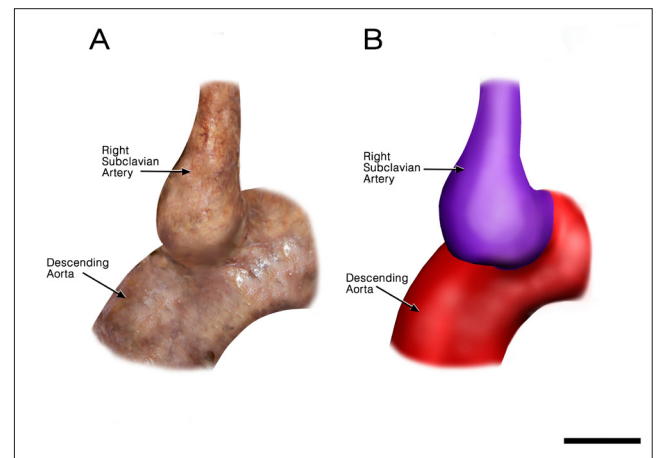


Figure 6. Photograph (A) and computer model (B) of the right subclavian artery with contiguous structures removed and viewed from the right lateral perspective. The origin of the vessel is atypically enlarged and it approximates the diameter of the descending aorta. Bar = 20 mm.

the proximal portion of the 4th arch diminishes and the brachiocephalic trunk fails to form. The proximal portions of the third arch do not involute and a singular outflow is retained as a bicarotid trunk. The adult specimen displays this characteristic arrangement that likely emerged, in part, as a result of defective involution of the distal fourth trunk (Animations 1,2).

Previous work utilizing experimental mouse models suggest that unique gene signaling in the fourth arch artery may make it more susceptible to interruption during early vascular development (Bergwerff et al., 1999). Studies using Tgf β 2 knockout mice showed that diminished TGF- β -SMAD2 signaling can lead to retroesophageal ARSA (Molin et al., 2004; Gittenberger-de Groot et al., 2006). SMAD2 signaling is localized to the smooth muscle cells of the fourth arch artery and has a role in regulating the expression of genes that encode fibronectin and neural cell adhesion molecule (Molin et al., 2004; Gittenberger-de Groot et al., 2006). Reduced TGF- β -SMAD2 signaling in this case may have interfered with the development of the vascular structure and innervation of the fourth arch leading to its unusual obliteration (Molin et al., 2004; Gittenberger-de Groot et al., 2006).

In addition to this, it has been hypothesized that hemodynamic variations, sensed by shear stress responsive genes like Tgf β 1, TBX-1 and Et-1, may have a role in arch variations as well (Poelmann et al., 2005). During angiogenesis and aortic arch remodeling, differences in blood flow through the vasculature either stimulate (low shear stress) or prevent (high shear stress) apoptosis of segments that are to be obliterated or retained, respectively (Keller et al., 2011; Poelmann et al., 2005). In the case of ARSA, reduced signaling by ET-1/ETA (Yanagisawa et al., 1998) and TGF- β -SMAD2, and perhaps reduced signaling by a number of other genes that are important in supporting and maintaining vascular structure and blood flow in the fourth arch, may lead to narrowing and abnormal apoptosis of this artery (Yanagisawa et al., 1998; Poelmann et al., 2005; Gittenberger-de Groot et al., 2006).

The proximal portion of the ARSA displayed a Kommerrell diverticulum. Although this feature was first discovered in a patient with an aberrant left subclavian artery, it frequently occurs in conjunction with ARSA. These patients typically report airway complications associated with tracheal and esophageal obstructions (Yang et al., 2012). It is also more likely that a fistula will develop between the ARSA and the esophagus likely due to the increased proximity and pressure between these two structures (Miller et al., 1996). However, the individual described here lacked a fistula and was apparently asymptomatic.

ARSA has been imaged within the clinical setting through various advanced methodologies (Meier et al., 1993; Turkenburg et al., 1994; Lee et al., 2004; Ilijevski et al., 2011). Although these volumetric renderings provide useful clinical information, they may not be optimal in an educational setting since contiguous structures such as the trachea and esophagus are not depicted. The approach used here combining photographic recordings with 3D computer

modeling facilitates ease-of-presentation (Stickley et al., 2013). The model can be viewed on virtually any laptop with color-coded structures. For example, the bulbous perimeter and surface of the ARSA with Kommerrell's diverticulum is easily visualized. Contiguous structures can be instantaneously removed from the scene enabling the student to investigate spatial relationships of the region such as retroesophageal position of the horizontal branch of the ARSA. Increased realism was achieved by viewing the model within the context of 3D projection with Z-space technology facilitating spatial relationships among the thoracic viscera.

Acknowledgements

The authors acknowledge the generous donation of the anatomical materials by an anonymous individual in the Willed Body Program, the University of Hawaii School of Medicine, Honolulu, HI.

Animations

Animation 1. Structures anatomically associated with aortic arch development in the Carnegie Stage 16 Human Embryo. Colors correspond with structures indicated in the figures. Black represents structures that normally regress.

http://www.ijav.org/2016/ijav_2016-055_animation-1.mov

Animation 2. Schematic transition of probable aortic arch branching pattern causing the ARSA (based on Sadler, 2012: 186). In the typical condition, the portion of the dorsal aorta distal to the right 7th intersegmental artery (presumptive right subclavian artery) regresses. The subclavian combines with the right common carotid and it is incorporated into the developing aortic arch to form the right innominate artery. In the atypical case, the dorsal aorta regresses proximal to the 7th intersegmental artery and the presumptive right subclavian artery is retained by the developing descending aorta and, thus, forms as a branch distal to the left 7th intersegmental artery (presumptive left subclavian branch). Simultaneously, the proximal portions of the right and left common carotid arteries retain with a singular stalk arising from the developing aortic arch.

http://www.ijav.org/2016/ijav_2016-055_animation-2.mov

Animation 3. ARSA in the adult cadaver depicting spatial relationships of the relevant cardiovascular structures including the presence of a bicarotid trunk, left subclavian artery and the ARSA arising as the terminal branch of the aortic arch and curving abruptly posteriorly and then superiorly as it gives rise to the right subclavian artery.

http://www.ijav.org/2016/ijav_2016-055_animation-3.mov

Animation 4. ARSA in the adult cadaver depicting retroesophageal and retrotracheal position of the right subclavian artery.

http://www.ijav.org/2016/ijav_2016-055_animation-4.mov

References

- Austin EH, Wolfe WG. 1985. Aneurysm of aberrant subclavian artery with a review of the literature. *J Vasc Surg.* 2:571-577.
- Bergman RA, Thompson SA, Afifi AK, Saadeh FA. 1988. *Compendium of Human Anatomic Variation.* Urban & Schwarzenberg, Munich, pp: 328-331.
- Bergwerff M, DeRuiter MC, Hall S, Poelmann RE, Gittenberger-de Groot AC. 1999. Unique vascular morphology of the fourth aortic arches: possible implications for pathogenesis of type-B aortic arch interruption and anomalous right subclavian artery. *Cardiovasc Res.* 44:185-196.
- Boas N, Desmoucelle F, Bernadt V, Franceschi JC. 2002. Rare cause of acute ischemia of the right upper extremity: Thrombosis of a retroesophageal subclavian artery. *Ann Vasc Surg.* 16:387-390.
- Brown DL, Chapman WC, Edwards WH, Coltharp WH, Stoney WS. 1993. Dysphagia lusoria: aberrant right subclavian artery with a Kommerell's diverticulum. *Am Surg.* 59:582-586.
- Chadha NK, Chiti-Batelli S. 2004. Tracheostomy reveals a rare aberrant right subclavian artery: a case report. *BMC Ear Nose Throat Disord.* 4:1.
- Chaoui R, Rake A, Heling KS. 2008. Aortic arch with four vessels: aberrant right subclavian artery. *Ultrasound Obstet Gynecol.* 31: 115-117.
- Congdon ED. 1922. Transformation of the aortic-arch system during the development of the human embryo. *Contributions to Embryology* 14:47-110.
- Davies M, Guest PJ. 2003. Developmental abnormalities of the great vessels of the thorax and their embryological basis. *Br J Radiol.* 76:491-502.
- Donnelly LF, Fleck RJ, Pacharn P, Ziegler MA, Fricke B, Cotton RT. 2002. Aberrant subclavian arteries cross-sectional imaging findings in infants and children referred for evaluation of extrinsic airway compression. *AJR Am J Roentgenol.* 178:1269-1274.
- Epstein DA, DeBord JR. 2002. Abnormalities associated with aberrant right subclavian arteries: a case report. *Vasc Endovascular Surg.* 36:297-303.
- Fazan VPS, Ribeiro RA, Ribeiro JAS, OAR Filho. 2003. Right retroesophageal subclavian artery. *Acta Cir Bras.* 18:54-56.
- Gittenberger-de Groot AC, Azhar M, Molin DG. 2006. Transforming growth factor β -SMAD2 signaling and aortic arch development. *Trends Cardiovasc Med.* 16:1-6.
- Ilijevski N, Nenezic D, Popov P, Sagic D, Radak D. 2011. Images in vascular medicine. Giant aneurysm of the aberrant right subclavian artery (arteria lusoria). *Vasc Med.* 16:157-158.
- Keller BB, Hoying JB, Markwald RK. 2011. Chapter 9. Molecular Development of the Heart. In: Fuster V, Walsh RA, Harrington RA (eds), *Hurst's, The Heart*, edition 13. McGraw-Hill, NY, 172-194.
- Knight L, Edwards JE. 1974. Right aortic arch: Types and associated cardiac anomalies. *Circulation.* 50:1047-1051
- Lee EY, Siegel MJ, Hildeboldt CF, Gutierrez FR, Bhalla S, Fallah JH. 2004. MDCT evaluation of thoracic aortic anomalies in pediatric patients and young adults: comparison of axial, multiplanar and 3D images. *AJR Am J Roentgenol.* 182: 777-784.
- Meier RA, Marianacci EB, Costello P, Fitzpatrick PJ, Hartnell GG. 1993. 3D image reconstruction of right subclavian artery aneurysms. *J Comput Assist Tomogr.* 17:887-890.
- Miller RG, Robie DK, Davis SL, Cooley DA, Klish WJ, Skolkin MD, Kearney DL, Jaksic T. 1996. Survival after aberrant right subclavian artery-esophageal fistula: Case report and literature review. *J Vasc Surg.* 24:271-275.
- Moes CA, Freedom RM. 1993. Rare types of aortic arch anomalies. *Pediatr Cardiol.* 14:93-101.
- Molin DG, Poelmann RE, DeRuiter MC, Azhar M, Doetschman T, Gittenberger-de Groot AC. 2004. Transforming growth factor β -SMAD2 signaling regulates aortic arch innervation and development. *Circ Res.* 95:1109-1117.
- Nakatani T, Tanaka S, Mizukami S, Okamoto K, Shiraishi Y, Nakamura T. 1996. Retroesophageal right subclavian artery originating from the aortic arch distal and dorsal to the left subclavian artery. *Ann Anat.* 178:269-271.
- Natsis KI, Tsiouridis IA, Didagelos MV, Fillipidis AA, Vlasis KG, Tsikaras PD. 2009. Anatomical variations in the branches of the human aortic arch in 633 angiographies: clinical significance and literature review. *Surg Radiol Anat.* 31: 319-323.
- O'Rahilly R. 1971. The timing and sequence of events in human cardiogenesis. *Acta Anat (Basel).* 79:70-75.
- Poelmann RE, Gittenberger-de Groot AC. 2005. Apoptosis as an instrument in cardiovascular development. *Birth Defects Res C Embryo Today.* 75:305-313.
- Rogers AD, Nel M, Eloff EP, Naidoo NG. 2011. Dysphagia lusoria: A case of an aberrant right subclavian artery and a bicarotid trunk. *ISRN Surg.* 2011: 819295.
- Sadler TW. 2012. *Langman's Medical Embryology.* Lippincott Williams & Wilkins, New York. 12th Ed., pp 185-191.
- Saito T, Tamatsukuri Y, Hitosugi T, Miyakawa K, Shimizu T, Oi Y, Yoshimoto M, Yamamoto Y, Spinel-Browski K, Steinke H. 2005. Three cases of retroesophageal right subclavian artery. *J Nippon Med Sch.* 72:375-382.
- Stickley CD, Tamura K, Labrash SJ, Lozanoff S. 2013. Bifurcation of the fourth rib as a possible indicator of Gorlin's Syndrome in an 85-year-old female cadaver. *Int J Anat Var (IJAV)* 6:86-89.
- Tubbs RS, Oakes WJ, Salter G, Zehren SJ. 2004. Retroesophageal right subclavian artery with persistent ductus arteriosus. *Anat Sci Int.* 79:98-100.
- Turkenburg JL, Versteegh MI, Shaw PC. 1994. Case report: aneurysm of an aberrant right subclavian artery diagnosed with MR imaging. *Clin Radiol.* 49:837-839.
- Yanagisawa H, Hammer RE, Richardson JA, Williams SC, Clouthier DE, Yanagisawa M. 1998. Role of Endothelin-1/Endothelin-A receptor-mediated signaling pathway in the aortic arch patterning in mice. *J Clin Invest.* 102:22-33.
- Yang C, Shu C, Li M, Li Q, Kopp R. 2012. Aberrant subclavian artery pathologies and Kommerell's diverticulum: A review and analysis of published endovascular/hybrid treatment options. *J Endovasc Ther.* 19:373-382.

